EurJOC
European Journal of Organic Chemistry

A Journal of
ChemPubSoc Europe

Accepted Article

Title: Selective room-temperature hydrogenation of carbonyl compounds under atmospheric pressure over platinum nanoparticles supported on ceria-zirconia mixed oxide

Authors: Elena Redina, Kseniia Vikanova, Gennady Kapustin, Igor Mishin, Olga Tkachenko, and Leonid Kustov

To be cited as: *Eur. J. Org. Chem.* 10.1002/ejoc.201900215

Link to VoR: http://dx.doi.org/10.1002/ejoc.201900215

Supported by
ACES Asian Chemical Editorial Society

WILEY-VCH

Selective room-temperature hydrogenation of carbonyl compounds under atmospheric pressure over platinum nanoparticles supported on ceria-zirconia mixed oxide

Elena A. Redina,* [a] Kseniia V. Vikanova,[a] Gennady I. Kapustin, [a] Igor V. Mishin, [a] Olga P. Tkachenko, [a] and Leonid M. Kustov [a, b]

Abstract: A Pt/CeO_2-ZrO_2 catalytic system was able to initiate an extremely intense hydrogen spillover providing a huge amount of activated hydrogen (12 mol/mol Pt) at temperatures -50ºC - +25ºC, which was not observed before. The idea was to use this activated hydrogen for reduction of carbonyl compounds under ambient conditions. Thus, the efficient and selective heterogeneous hydrogenation of carbonyl compounds of different structure, including 5-hydroxymethylfurfural and cinnamaldehyde, to the corresponding alcohols with quantitative yields was successfully performed over the Pt/CeO_2-ZrO_2 catalysts at room-temperature and atmospheric pressure of H_2. The proposed catalysts afforded hydrogenation under significantly milder conditions with a much higher activity and selectivity compared to the commercial catalysts and reported catalytic systems. Hydrogenation of the C=O bond in the presence of a C=C bond proceeded with a high regioselectivity.

Introduction

Carbonyl compounds are abundant natural products, and their reduction to the corresponding alcohols plays an important role in modern organic chemistry, especially in drug design, totaling 9% of the whole pool of reactions used in pharmaceutical synthesis [1]. The common synthetic approach to obtain target alcohols from aldehydes and ketones still implies the use of stoichiometric reducing agents, such as $LiAlH_4$ [2] or boranes [4],[5], which are hazardous and produce wastes. Despite the fact that hydrogenation without the use of stoichiometric reductants is the high-priority process in the list of key Green Chemistry research areas and many efforts have been made to overcome the problem, there is still a big room for improvements in developing alternative methods for hydrogenation by molecular hydrogen [6]. Homogeneous catalysis represents an alternative “greener” way for the reduction of carbonyl compounds to alcohols with H_2 acting as a benign reducing agent [7]-[10]. However, there are still such drawbacks as difficulties of catalyst isolation and separation, its poor recyclability. In addition, rather severe conditions are usually required for the process to proceed with a good product yield. Recently, Tan et al. showed that Ru(II) complexes were highly active in aldehyde hydrogenation. Even so, a high H_2 pressure and elevated temperatures were needed, and the reaction proceeded for 24 h to obtain alcohols in good yields [7] (Scheme 1 A). The Triphos-Ru(CO)H_2 complex was also used for aldehyde hydrogenation, but high temperatures (100-140ºC) and pressures (30 bar) were required [10]. Lately, Wei et al. hydrogenated a wide range of ketones over a Re-containing complex; yet, the presence of a base, harsh conditions and long reaction time were necessary to achieve high conversions [9] (Scheme 1 B).

At the same time, heterogeneous hydrogenation can be more convenient in use, and it is able to overcome the problems associated with homogeneous catalysis [11]-[14]. Even so, heterogeneous catalysts are usually considered as less selective toward C=O bond hydrogenation in the presence of other easily reducible groups, such as a C=C bond. Nevertheless, recently, Tamura et al. performed selective hydrogenation of unsaturated ketones to unsaturated alcohols with good yields over Ir/MgO catalysts. However, the reaction was conducted at a high H_2 pressure and a high molar amount of Ir [12] (Scheme 1 C).

Platinum is known as the most active metal for hydrogenation reactions. Pt catalysts were successfully applied in liquid-phase selective hydrogenation of aldehydes and ketones to the corresponding alcohols [15]-[19], even to the unsaturated ones [20]-[23]. Nevertheless, to achieve the desired product in a good yield, a high H_2 pressure and temperature are also required, which leads to the necessity in high-pressure equipment [19], [21] (Scheme 1 D, E). Though the reaction can be performed at ambient conditions, a large amount of Pt is needed and the reaction proceeds too long [17], [20] (Scheme 1 F), which increases substantially the cost of the process and product. Therefore, the design of novel heterogeneous catalysts for the hydrogenation of carbonyl compounds with a high activity, selectivity, predictable behavior and ability to work under mild conditions is still a big challenge for scientists.

---

[a] Dr E. Redina, K. Vikanova, Dr. G. Kapustin, Dr. Prof. I. Mishin, Dr. O. Tkachenko, Dr. Prof. L. Kustov
Laboratory of Development and Study of Polyfunctional Catalysts
Zelinsky Institute of Organic Chemistry RAS
119991, Leninsky pr., 47, Moscow, Russian Federation
E-mail: redinalena@yandex.ru
www.zioc.ru
[b] Dr. Prof. L. Kustov
Chemistry Department
Lomonosov Moscow State University
119991, Leninskie gory, 1, Moscow, Russian Federation

Supporting information for this article is given via a link at the end of the document.

10.1002/ejoc.201900215

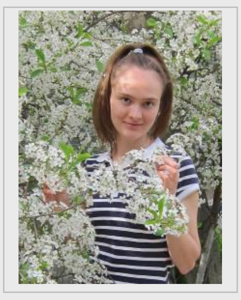

Dr. Redina Elena is a scientific researcher in the Laboratory of polyfunctional catalysts of Zelinsky Institute of Organic Chemistry. She defended her PhD thesis under supervision of Prof. Leonid Kustov in 2015. Her research interests are focused on preparation of new heterogeneous catalysts and their application in organic synthesis. The area of her research work covers catalysis by gold, green chemistry, oxidation and reduction processes. She has over 15 publications and more than 20 theses.

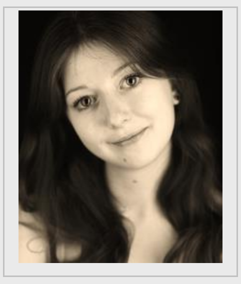

Vikanova Kseniia graduated the M.V. Lomonosov Moscow State University of Fine Chemical Technologies, Russia, department of Petrochemical synthesis and synthetic liquid fuel with a master's degree in 2016. Currently she is carrying out a PhD research in the Laboratory of polyfunctional catalysts at N.D. Zelynsky Institute of Organic Chemistry RAS. Her work is focused on the synthesis of heterogeneous catalysts and their testing in the reactions of selective carbonyl and nitro compounds hydrogenation.

Dr. Kapustin Gennady is a senior research associate of the Laboratory of Polyfunctional Catalysts of N.D.Zelinsky Institute of Organic Chemistry Russian Academy of Sciences since 1971. His research interests include catalyst characterization by adsorption, adsorption calorimetry and temperature-programmed techniques (TPD, TPR, TPO). He is a co-author of more than 70 papers.

Prof., Dr. Igor Mishin is a leading scientific researcher of the Laboratory of Polyfunctional Catalysts of N.D.Zelinsky Institute of Organic Chemistry. He is a specialist in surface science and X-ray difraction analysis. He is a co-author of more than 100 publications.

Dr. Tkachenko Olga works for Zelinsky Institute of Organic Chemistry (Russian Academy of Sciences) from 1966 up to now. She received Ph. Degree in 1978. From 1986 she was employed as the scientific researcher. Since 1990 - up to now - as a senior researcher. Dr. Tkachenko is high class expert in field of catalysts study by modern physicochemical methods. The scope of her interest is the surface properties and local structure of heterogeneous catalysts. She has 32 Oral and 90 Poster Presentations at Scientific Conferences and 169 Publications.

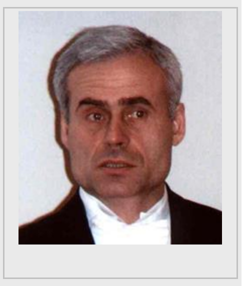

Prof., Dr. Kustov Leonid is the Head of the Laboratory of Development of Polyfunctional Catalysts at the N.D. Zelinsky Institute of Organic Chemistry, the Head of Laboratory of Nanochemistry and Ecology at National University of Science and Technology MISiS, and the Head of Laboratory of Ecological Chemistry at Chemistry Department of Moscow State University. He is an expert in the areas of physical chemistry, catalysis and nanomaterials. He coauthored over 500 papers and about 80 patents

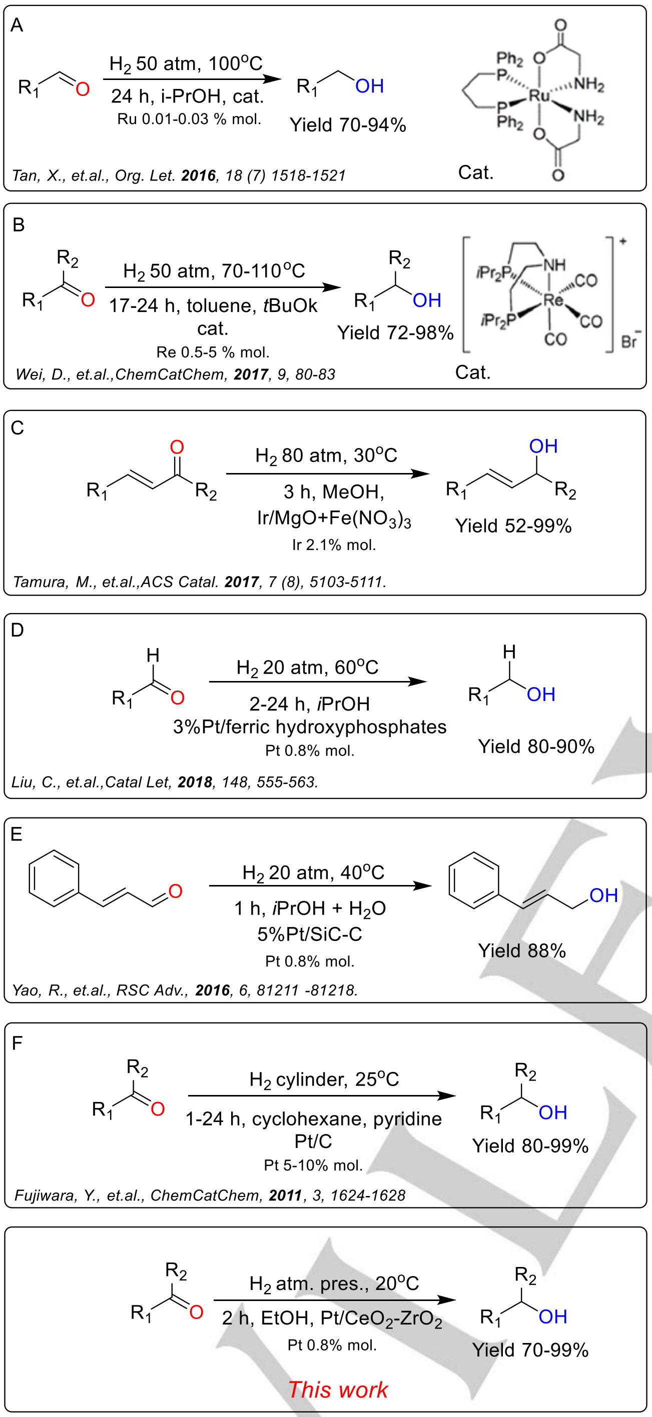

Scheme 1. Advances in homogeneous and heterogeneous catalytic hydrogenation of carbonyl compounds and results obtained in this work.

In this work, we propose CeO_2 based Pt catalysts for hydrogenation of carbonyl compounds. The interaction of supported Pt nanoparticles (NPs) with reducible oxides, such as CeO_2, leads to partial oxide reduction (M^{4+}→M^{3+}) [24]-[26] with formation of new catalytic sites, where the carbonyl bond can be activated [27]-[28]. At the same time, the reducibility of CeO_2 can be significantly improved by its doping with suitable elements. Ceria doped with ZrO_2 is characterized by enhanced redox conversion Ce^{4+}→Ce^{3+} [29]-[31]. Thus Pt NPs supported on Ce-Zr mixed oxides seem to be a prominent system for C=O bond activation and its further hydrogenation.

Recently, we showed that Pt supported on ceria-zirconia mixed oxide provide hydrogenation of nitro aromatic compounds to anilines under room temperature and atmospheric pressure [32]. Here we report on Pt nanocatalysts supported on CeO_2-ZrO_2 oxide for the selective hydrogenation of carbonyl compounds either at room temperature or below 0°C in an H_2 atmosphere under ambient pressure (Scheme 1). The novelty of the present work is the combination of high activity and selectivity typical for homogeneous catalysis and easy-to-handle heterogeneous catalysis, which can operate just at ambient conditions as enzymes in living organisms. This becomes possible due to dual activity of Pt NPs and active oxide support via the hydrogen spill over effect. The reduction behaviour of the prepared catalysts and their activity in the hydrogenation reaction were evaluated with the use of a simple TPR-H_2 method.

Results and Discussion

The XRD pattern of the CeO_2-ZrO_2 sample calcined at 400°C (Fig. S2, SI) showed reflections of CeO_2 with the cubic structure, cell parameter a=5.41 Å, and the average crystallite size 5 nm. No reflections of ZrO_2 were observed that could be attributed to its amorphous state in the sample. Thus, CeO_2 and ZrO_2 form two separate phases without formation of a solid solution, which was additionally checked by calcination of the CeO_2-ZrO_2 sample at 900°C. The XRD pattern of the sample calcined at 900°C showed solely the reflection of cubic CeO_2 with no changes in the cell parameter and average particle size 20 nm (Fig.S4, SI). The SEM-EDS analysis of the obtained support revealed a uniform distribution of Zr, Ce, and O in the sample (Fig. S7, SI).

The TEM study of the 1%Pt/CeO_2-ZrO_2 sample showed rather uniform Pt NPs size distribution with an average size about 2 nm (Fig. S8, SI). The similar particle size distribution was observed for 1Pt/CeO_2 (for TEM image, see Fig. S9-S11, SI). However, the TEM results were not fully reliable because oxide supports CeO_2-ZrO_2, CeO_2, ZrO_2 showed low Z-contrast to Pt NPs. Moreover, the obtained oxides are highly dispersed, and for Pt/CeO_2-ZrO_2 sample there are two types of NPs supported on CeO_2: Pt and ZrO_2, which makes it difficult to identify them by means of TEM only. Thus, in this case we applied CO chemisorption technique to calculate the size of Pt NPs. According to CO adsorption data the mean particle size of Pt NPs in 1%Pt/CeO_2-ZrO_2, 1%Pt/CeO_2 and Pt/ZrO_2 is close to 2 nm (1.98, 1.94 and 2.10 nm respectively) (Table S2.1, SI).

The TPR-H_2 study of supports revealed an easier reduction of CeO_2-ZrO_2 mixed oxide with enhanced H_2 consumption compared to CeO_2 and ZrO_2 samples (Fig. 1). The bulk reduction of Ce^{4+} to Ce^{3+} proceeded at a lower temperature (718°C) compared to the temperatures of bulk reduction of pure CeO_2 (>800°C), while the surface reduction of CeO_2 proceeded at

500°C for both samples. However, the surface reduction of CeO_2-ZrO_2 mixed oxide is accompanied by the reduction of ZrO_2, which proceeds at 300-800°C with a maximum at 450°C.

The low-temperature reduction peak for CeO_2-ZrO_2 with a maximum at 350°C could be associated with reduction of the dispersed CeO_2 phase (Fig. 1).

The easier reduction of the ceria-zirconia oxides is usually attributed to the Zr incorporation in the CeO_2 crystal lattice, which causes distortion of the M-O bond symmetry due to solid solution formation with induced oxygen ion conductivity [33]-[34].

As we did not reveal the formation of a solid solution $Ce_{0.8}Zr_{0.2}O_2$, the easier reduction of CeO_2-ZrO_2 compared to CeO_2 and ZrO_2 can be explained in terms of grain-boundary diffusion of oxygen induced by a high density of defects on the boundaries of ZrO_2 and CeO_2 nanocrystallites [35]-[36].

Outstanding results were observed in the TPR-H_2 study of Pt catalysts. For the reduced Pt/CeO_2 and Pt/CeO_2-ZrO_2 samples, hydrogen consumption has already started at -50°C (Fig. 2A). Moreover, the molar hydrogen uptake values in the range from -50 to +25°C for the reduced 1%Pt/CeO_2-ZrO_2 sample was twelve times higher than the molar Pt content, i.e. 269 L H_2/mol Pt (Fig. 2A). For the 1%Pt/CeO_2 sample, hydrogen consumption reached only a modest value of 2.6 mol H_2/mol Pt (Fig. 2A). Yet, negligible hydrogen adsorption was observed for Pt NPs supported on non-reducible oxides, i.e. for both 1%Pt/ZrO_2 and 1%Pt/SiO_2 (taken as a reference sample, for characterization see Supp. Info) the H_2/Pt molar ratio was 0.3. Such differences can be explained by the nature of the support, while the BET surface area and Pt NPs size distribution were almost the same for all the samples.

Hydrogen desorption in an Ar flow was also observed for 1%Pt/CeO_2 and 1%Pt/CeO_2-ZrO_2 samples (Fig. 2B). The maxima of the desorption peak are located at 54 and 45°C, respectively. The amount of hydrogen desorbed was three times higher for the catalyst supported on CeO_2-ZrO_2 mixed oxide than for the CeO_2 supported catalyst.

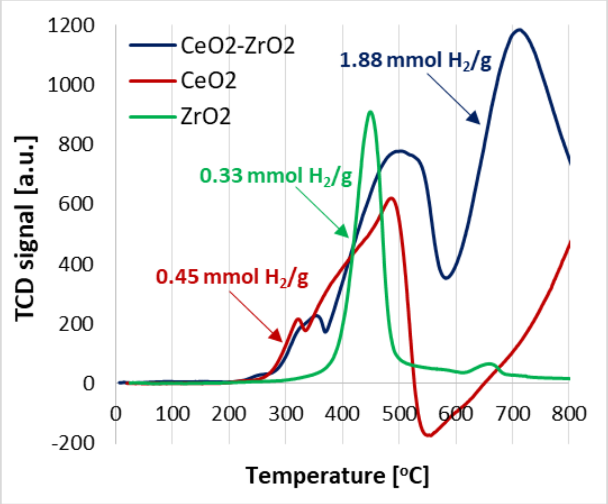

Figure 1. TPR-H_2 study of supports (CeO_2, ZrO_2, CeO_2-ZrO_2) and calculated H_2 uptake for each sample.

The unusual features of the 1%Pt/CeO_2-ZrO_2 and 1%Pt/CeO_2 catalysts can be attributed to the low-temperature hydrogen spillover effect [37]-[41]. The desorption experiment also indicated the hydrogen spillover known to be in equilibrium with reverse hydrogen spillover from the metal oxide support to supported metal NPs [39], [42].

Lykhach et el. observed the hydrogen spillover over a model system Pt/CeO_2 (111)/Cu(111) using resonant photoemission spectroscopy in UHV by registering the change in the electronic state from Ce^{4+} to Ce^{3+} at temperatures -90-13°C [41]. Non-stoichiometric excessive hydrogen consumption of 3-4.8 H_2/Pt mol/mol was observed in [43], [44] on a $Ce_{0.99}Pt_{0.01}O_2$ system at temperatures -40- +80°C, yet the platinum in the sample was in the Pt^{2+} state. For reduced Pt/$CeZrO_2$ systems, hydrogen consumption at RT (25°C) did not exceed H_2/Pt 0.5 mol/mol [45], [46].

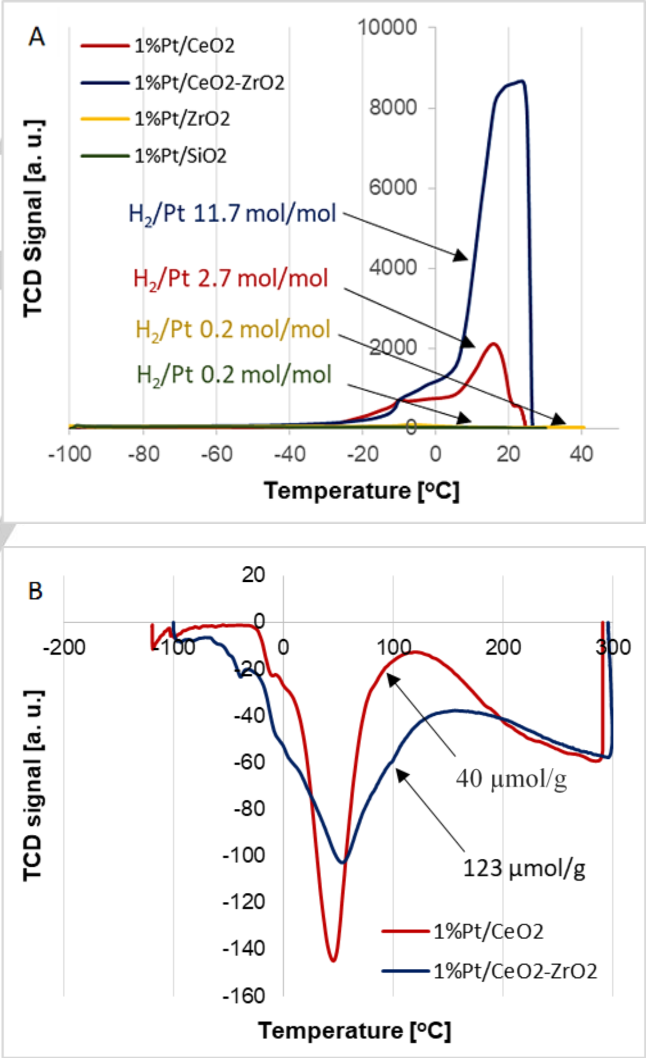

Figure 2. TPR-H_2 study of reduced Pt catalysts on different oxide supports and calculated specific H_2 consumption (mol H_2/mol Pt) for each sample (A); TPD-H_2 study on reduced Pt/CeO_2 and Pt/CeO_2-ZrO_2 catalysts (B).

10.1002/ejoc.201900215

Thus, to the best of our knowledge, in the present work for the first time we observed such an extreme hydrogen consumption at temperatures far below 0ºC and near RT, which indicated the active hydrogen spillover.

Further, our idea was to use this unique hydrogen activation ability of Pt NPs supported on CeO_2-ZrO_2 mixed oxide in selective hydrogenation of carbonyl compounds under ambient and sub-ambient temperatures. The hydrogenation reaction was performed in a glass two-necked flask. Before the reaction started, the catalyst was placed in the reactor and pretreated under an H_2 flow at the reaction temperature (-15 - +20ºC) for 30 min. After that, the H_2 flow was switched off and the substrate diluted with a solvent was added through the sample valve. The reaction proceeded at a desired temperature (-15 - +20ºC) in H_2 under atmospheric pressure.

The reaction conditions were optimized in hydrogenation of 1-hexanal to 1-hexanol as hydrogenation of aliphatic aldehydes usually is more difficult than that of the aromatic ones and it is logical to perform optimization of the reaction using less reactive substrates (Table 1). In all cases, the selectivity to the alcohol was 100% and the extent of conversion was different in the experiments under varied conditions or the catalyst used, which led to different yields of 1-hexanol. The solvent did not have any significant influence on the yield of 1-hexanol over 1%Pt/CeO_2-ZrO_2, and EtOH was chosen as a “greener” option (Entries 1-3). The 1%Pt/CeO_2-ZrO_2 catalyst appeared to be more active than 1%Pt/CeO_2 giving the yield of 1-hexanol 74% against 50% (Entries 1 and 8, respectively), while the yield of 1-hexanol on 1%Pt/ZrO_2 and 1%Pt/SiO_2 achieved 32-35%. This is the evidence that the reaction can proceed on Pt itself as for the catalysts on non-reducible oxides. But for Pt on CeO_2 and CeO_2-ZrO_2, the carrier starts to play a crucial role in the activity of the catalysts in the hydrogenation reaction.

Moreover, performing the reaction over 1%Pt/CeO_2-ZrO_2 at -2ºC has not sufficiently decreased the yield of 1-hexanol giving 65% instead of 75% (Entries 1 and 4). Even at -15ºC, the yield of 1-hexanol was 25% and significantly exceeded the yield observed on a commercial 1%Pd/C catalyst by 8 times (Entries 5-6). Thus, our idea worked, and the prepared Pt/CeO_2-ZrO_2 catalyst was able to operate even under sub-ambient conditions, i.e. in the temperature range where the extreme hydrogen spillover was observed.

The catalyst 0.5%Pt/CeO_2-ZrO_2 showed almost the same activity as 1%Pt/CeO_2-ZrO_2, and after 4 h the complete conversion of 1-hexanal was observed with the 1-hexanol yield > 99% (Entries 11-12). However, the sample 0.025%Pt/CeO_2-ZrO_2 was not active under the conditions used. These results completely correlate with the data obtained by the TPR study. The low-temperature activity in 1-hexanal hydrogenation was observed, if low-temperature hydrogen spillover was revealed by TPR. Though there were small differences in the behavior of 1%Pt/CeO_2-ZrO_2 and 0.5%Pt/CeO_2-ZrO_2 under the TPR experiment and almost the same H_2/Pt molar ratio was observed at temperatures -50-+25ºC for both samples (See Supp. Info., Fig. S4), the H_2 consumption by the 0.025%Pt/CeO_2-ZrO_2 catalyst started only at 50ºC (See Supp. Info., Fig. S6). Thus, the 0.025%Pt/CeO_2-ZrO_2 sample did not show activity in hydrogenation of 1-hexanal under the ambient conditions used (Entry 13).

Recycling of 1%Pt/CeO_2-ZrO_2 showed that the conversion of 1-hexanal was not quite stable from run to run finally achieving a constant value of 27% if the catalyst was not washed before each repeated test. However, washing the catalyst with acetone and water after the second use completely restored its activity (Fig. 3). Blocking the catalyst surface with adsorbed substrates and products may prevent hydrogen adsorption while preactivating the catalyst in an H_2 flow and the catalyst gradually looses its activity; thus, washing the catalysts is needed to remove the adsorbed species.

Table 1. The conditions of 1-hexanal hydrogenation.

Entry	Catalyst	Pt [% mol.]	Solvent	t [ºC]	Time [h]	Yield [%] [a]
1	1%Pt/CeO_2-ZrO_2	0.85	EtOH	20	2	75
2	1%Pt/CeO_2-ZrO_2	0.85	*i*PrOH	20	2	74
3	1%Pt/CeO_2-ZrO_2	0.85	hexane	20	2	70
4	1%Pt/CeO_2-ZrO_2	0.85	EtOH	-2	2	65
5	1%Pt/CeO_2-ZrO_2	0.85	EtOH	-15	2	25
6	1%Pd/C-commercial	0.85	EtOH	-15	2	3
7[b]	1%Pt/CeO_2-ZrO_2	0.085	EtOH	-2	2	11
8	1%Pt/CeO_2	0.85	EtOH	20	2	50
9	1%Pt/ZrO_2	0.85	EtOH	20	2	35
10	1%Pt/SiO2	0.85	EtOH	20	2	32
11	0.5%Pt/CeO_2-ZrO_2	0.43	EtOH	20	2	67
12	0.5%Pt/CeO_2-ZrO_2	0.43	EtOH	20	4	>99
13	0.025%Pt/CeO_2-ZrO_2	0.022	EtOH	20	2	6

Reaction conditions: 1-hexanal (0.3 mmol), catalyst (50 mg), solvent (1.5 ml), 2-4 h, H_2 medium. [a] determined by GC. [b] catalyst 5 mg.

Further we have extended the list of substrates. Aliphatic aldehydes were hydrogenated to the corresponding alcohols with quantitative yields in 2-4 h (Table 2, entries 1-2). Hydrogenation of benzaldehyde to benzyl alcohol also proceeded with a quantitative yield (Table 2, entry 3). Para- and meta-substituted benzaldehydes with π-electron-donating groups can also be effectively hydrogenated to the corresponding alcohols with yields > 99 % (Table 2, entries 4-5, 8-9). When hydrogenating p-chloro-substituted benzaldehyde, the selectivity decreased to 75% because of a hydrodechlorination process and benzyl alcohol was obtained along with the target product (Table 2, entry 6). Meanwhile, p-fluorobenzaldehyde was hydrogenated to the corresponding alcohol with the quantitative yield (Table 2, entry 7). 2-Formylpyridine can also be effectively hydrogenated in 3.5 h (Table 2, entry 10).

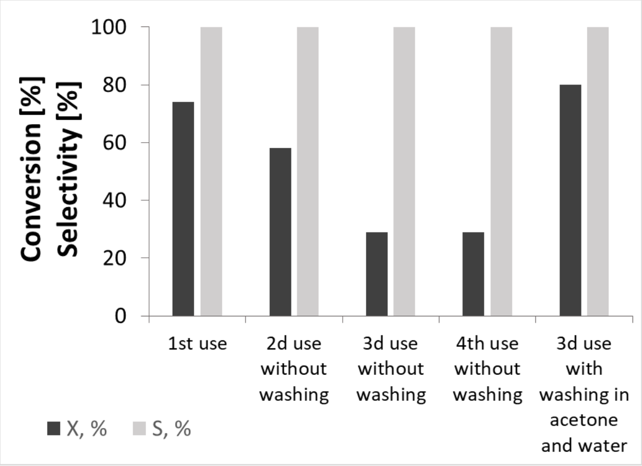

Figure 3. Recyclability of the 1%Pt/CeO_2-ZrO_2 catalyst in 1-hexanal to 1-hexanol hydrogenation. X – conversion, S – selectivity.

We checked the TOFs of hydrogenation of p-substituted benzaldehyde with electron-donating (EDG) and electron-withdrawing (EWG) groups (Table 3). The rate of substrate hydrogenation decreased in the following order: p-fluorobenzaldehyde > benzaldehyde > p-methoxybenzaldehyde > p-(dimethyl)aminobenzaldehyde.

Table 2. Hydrogenation of aldehydes over 1%Pt/CeO_2-ZrO_2.

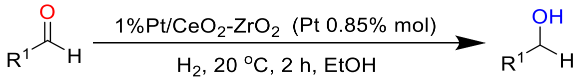

Entry	Substrate	Product	X [%][b]	S [%][b]	Yield [%][c]
1[a]	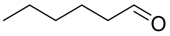	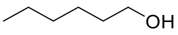	>99	100	n.d.
2	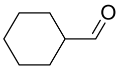	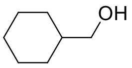	>99	100	>99
3	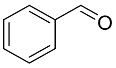	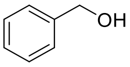	>99	100	>99
4	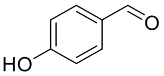	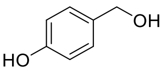	>99	100	>99
5	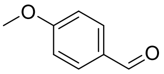	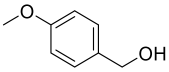	>99	100	>99
6	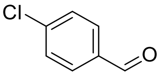	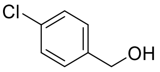	93	75	68
7	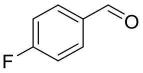	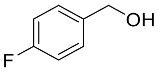	>99	100	>99
8	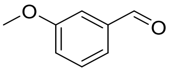	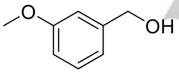	>99	100	>99
9	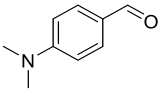	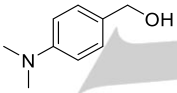	>99	100	>99
10 [d]	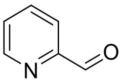	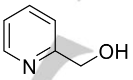	93	100	-
11	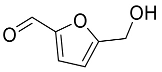	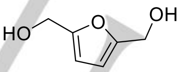	83 97[e]	100 100	n.d. 92 [e]
12	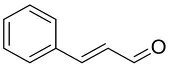	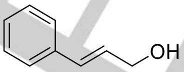	18	62	n.d.
13[f, g]	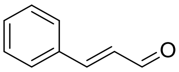	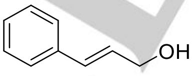	96	84	81
14 [f, g]	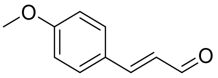	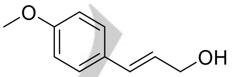	96	85	82

Reaction conditions: substrate (0.3 mmol), catalyst (50 mg, Pt 0.85% mol.), EtOH (1.5 ml), 2 h, 20°C, H_2 medium. [a] After 4 h. [b] Determined by GC. [c] Isolated yield, the purity was confirmed by ^1H and ^{13}C NMR (See Supp. Info S11-S32). [d] After 3.5 h. [e] The conversion and isolated yield after 3 h. [f] A NaOH aqua solution (1M) was added (6% mol.). [g] The NMR yield with dimethyl terephthalate used as an internal standard, the compounds were isolated and the purity was confirmed by ^1H and ^{13}C NMR (See Supp. Info Figs. S25-S28). X – conversion, S – selectivity, n.d. – not determined.

Thus, the stronger the ED-group in the para-position of benzaldehyde, the lower the reactivity of a substrate in hydrogenation; the presence of EW-groups in the para-position led to an increased substrate reactivity. This dependence is common for nucleophilic hydrogenation of carbonyl compounds with stoichiometric reducing agents, i.e. $NaBH_4$, $LiAlH_4$.

Extraordinary activity and selectivity were obtained in the case of hydrogenation of the bio-based platform molecule - 5-hydroxymethylfurfural (5-HMF). Hydrogenation of 5-HMF gives an extremely important product for modern polymer industry, namely 2,5-bis(hydroxymethyl)furan (BHMF), with the isolated yield 92% after 3 h (Table 2, entry 11) just at RT in an H_2 medium, which has not been done before even with the use of noble metal containing catalysts [47]-[52].

Table 3. Initial rate of p-substituted benzaldehyde hydrogenation.

Entry	Substrate	TOF [h^{-1}]
1	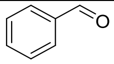	581
2	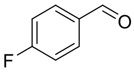	1406
3	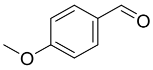	267
4	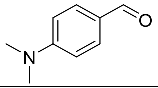	145

Reaction conditions: substrate (1 mmol), catalyst (28 mg, Pt 0.14% mol.), EtOH (1.5 ml), 15 min, 20°C, H_2 medium. TOF was calculated as the amount of the converted substrate (mol) per the amount of surface Pt (mol) per 0.25 h (TOF=$n_{\text{conv. sub}}/(n_{\text{Pt}}\cdot D\cdot t)$).

α,β-Unsaturated aldehydes were hydrogenated to the corresponding α,β-unsaturated alcohols with a high chemoselectivity in the presence of a catalytic amount of NaOH (Table 2, entries 12-14). Cinnamyl alcohol and p-methoxycinnamyl alcohol were obtained with the yields 81% and 82%, respectively, after 2 h (Table 2, entries 13-14). We compared TON values calculated for 1%Pt/CeO_2-ZrO_2, 1%Pt/CeO_2 and 1%Pt/ZrO_2 after 15 min of the reaction for. The obtained TONs were about 25000 for 1%Pt/CeO_2-ZrO_2 against 18500 for 1%Pt/CeO_2, while activity of 1%Pt/ZrO was negligible (TON value was 26), which indicated a much higher chemoselectivity of mixed oxide supported Pt catalysts, even though the characteristics of these three samples were almost the same (Table S2.1., SI). In addition, the results obtained for the Pt/CeO_2-ZrO_2 catalyst exceeded those reported in the literature: the reaction usually proceeded under more severe conditions at temperatures 60-150°C, pressures 10-40 bar and/or using a high Pt content with a selectivity to cinnamyl alcohol ranging within 40-90% [11], [53]-[63].

Worth noting that the Pt/CeO_2-ZrO_2 catalyst is an easily storable. We have shown that after a year of shelf life, it exhibits the same activity and selectivity in cinnamaldehyde hydrogenation to cinnamyl alcohol as a freshly prepared sample (Table S2, entry 3, SI).

We explored the activity of the synthesized catalysts in hydrogenation of ketones starting with acetone. Isopropyl alcohol was obtained quantitatively in 2 h in water (Table 4, entry 1). Aromatic ketones can also be hydrogenated to the corresponding secondary alcohols with quantitative yields, yet the time of the reaction for substituted aromatic ketones was prolonged to 5 h to obtain the complete substrate conversion. First, we checked the activity of the Pt/CeO_2 sample in hydrogenation of acetophenone and the conversion reached only 30% after 2 h (Table 4, entry 2). On the Pt/CeO_2-ZrO_2 catalyst, acetophenone was completely hydrogenated to 1-phenylethanol quantitatively in 2 h (Table 4, entry 3), while the Pt dispersion and other morphological characteristics of Pt/CeO_2 and Pt/CeO_2-ZrO_2 were the same. The isolated yield of 1-(4-methoxyphenyl) ethanol was >99% in 5 h (Table 5, entry 4); p-methylacetophenone was also hydrogenated quantitatively (Table 4, entry 5). Hydrogenation of p-diacetylbenzene with an electron-withdrawing substituent led to complete reduction of both carbonyl groups (Table 4, entry 6). 1-(2-hydroxyphenyl) ethanol was also obtained in a quantitative yield (Table 4, entry 6). The applied conditions led to hydrogenation of both nitro- and ketone groups in p-nitroacetophenone with the 1-(3-aminophenyl) ethanol yield of 98% (Table 4, entry 8) in 5 h. Hydrogenation of 2-acetylnaphthalene led to 1-(2-naphthyl) ethanol formation with the quantitative yield as well (Table 4, entry 9).

Table 4. Hydrogenation of aromatic ketones over 1%Pt/CeO_2-ZrO_2.

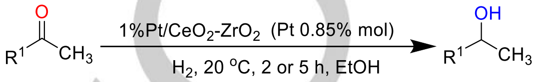

Entry	Substrate	Product	Yield [%] [a]
1	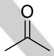	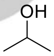	96 [b]
2[c, d]	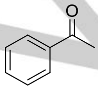	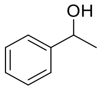	30
3[c]	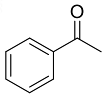	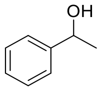	>99
4	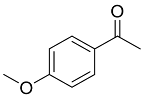	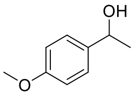	>99
5	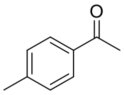	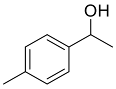	>99
6	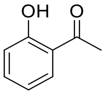	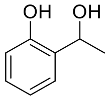	>99
7[e]	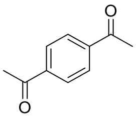	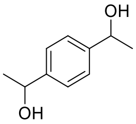	>99
8	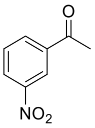	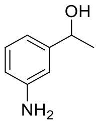	98
9	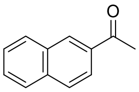	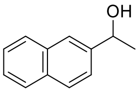	>99

Reaction conditions: substrate (0.3 mmol), catalyst (50 mg, Pt 0.85% mol.), EtOH (1.5 ml), 5 h, 20°C, H_2 medium. [a] Isolated yield, the purity was confirmed by ^1H and ^{13}C NMR (See Supp. Info. Figs.S33-S46). [b] GC yield. [c] 2 h. [d] catalyst: 1%Pt/CeO_2 (50 mg, Pt 0.85% mol.). [e] Reaction was performed in THF (1.5 ml).

To elucidate the possible scheme of hydrogenation of carbonyl compounds, we carried out an additional experiment on hydrogenation of acetone as a test molecule over different catalysts in water. According to NMR spectra recorded in an H_2O/D_2O solvent, the activity of acetone hydrogenation to iso-propanol (i-PrOH) increased in the following order: 1%Pt/SiO_2<1%Pt/ZrO_2<1%Pt/CeO_2<1%Pt/CeO_2-ZrO_2 (Fig. 4).

The calculated amount of i-PrOH formed is given in Table 5. While negligible conversion of acetone was observed over the Pt catalyst supported on non-reducible SiO_2, Pt NPs supported on the mixed oxide CeO_2-ZrO_2 support showed almost complete acetone conversion to i-PrOH (96%).

To understand the surface chemistry of acetone adsorbed on different catalysts, DRIFT spectra were recorded in two modes: 1) acetone adsorbed on the surface of the evacuated samples; 2) acetone adsorption was performed after hydrogen adsorption (40 Torr, 30 min) on pre-evacuated catalysts for 5 min or 17 h. It should be noted, that during acetone adsorption on oxide supports, several surface species could be observed: acetone molecules coordinated through the C=O bond, enolate species, which can be further transformed through an acid-base catalyzed aldol condensation to diacetyl alcohol (DAA) and mesityl oxide (MO) [64]-[66].

The obtained IR spectra significantly differed for the catalysts studied; and this is in coincidence with their catalytic activity. After 5 min of acetone adsorption in both modes, one can observe several bands in the range of 1500-1800 cm^{-1}, the position and intensity of these bands being dependent on the sample nature (Fig. 5-7). In all cases, the bands observed at 1750-1650 cm^{-1} were attributed to stretching vibrations of C=O in acetone molecules [64], [65], indicating that adsorption of acetone proceeds through the carbonyl group.

Acetone adsorbed on the least active catalyst 1%Pt/SiO_2 without pre-adsorbed hydrogen shows intense bands at 1714 cm^{-1} assigned to H-bonded acetone molecules and bands at 1620, 1561 cm^{-1}, which can be assigned to minority of DAA (1620 cm^{-1}) and adsorbed enolate forms of acetone (1561 cm^{-1}) [64], [66]. IR bands of acetone adsorbed on pure SiO_2 were much less intensive than on the Pt/SiO_2 catalyst, mostly C=O stretching vibrations of acetone having been observed (Fig. 6). After hydrogen adsorption on 1%Pt/SiO_2, the intensity of IR bands significantly reduced (Fig. 6). This could be because acetone is mostly adsorbed on the Pt NPs surface and the lesser amount is adsorbed on the SiO_2 surface as we can judge from the spectra recorded on pure SiO_2 (Fig. 6). The intensity and band position in the spectra recorded for Pt/SiO_2 (after H_2 adsorption) and SiO_2 (with or without pre-adsorbed hydrogen) are comparable either after 5 min or overnight exposure in acetone vapor (Fig. 6 A, B). Thus, we can conclude that hydrogen and acetone adsorb on the same sites on Pt NPs in Pt/SiO_2 catalysts and concurrent adsorption is observed, which leads to a low activity of these catalysts in the hydrogenation reaction.

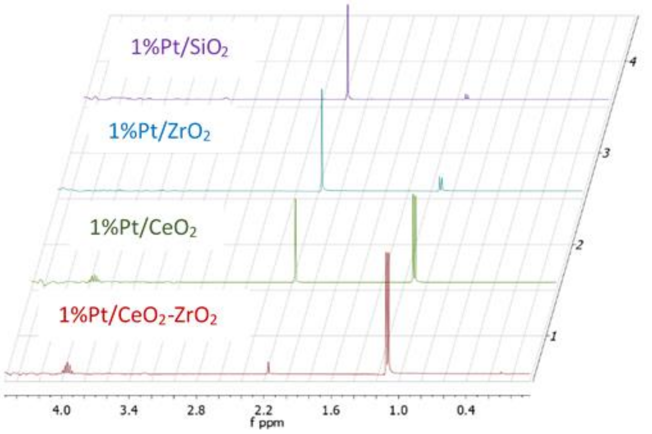

Figure 4. ^1H NMR spectra of the reaction mixture after acetone hydrogenation in water (2 h) on different catalysts.

Table 5. Acetone hydrogenation in water on different catalysts

Entry	Catalyst	X [%]
1	1Pt/CeO_2-ZrO_2	96
2	1Pt/CeO_2	69
3	1Pt/ZrO_2	29
4	1Pt/SiO_2	7

Reaction conditions: substrate (0.3 mmol), catalyst (50 mg, Pt 0.85% mol.), H_2O (1.5 ml), 2 h, 20°C, H_2 medium.

Quite a different picture was observed for the most active catalyst 1%Pt/CeO_2-ZrO_2 (Fig. 7). There are bands at 1709, 1690, 1627, and 1573 cm^{-1} in the spectra after 5 min of acetone adsorption on the surface of pre-evacuated Pt/CeO_2-ZrO_2 and CeO_2-ZrO_2 mixed oxide (Fig. 7 A). The first two bands are ascribed to stretching vibrations of C=O in acetone molecules interacting with L-sites, while the band at 1627 cm^{-1} could be ascribed to DAA and the band at 1573 cm^{-1} can correspond to carboxylate species, when the carbonyl group is coordinated to L-sites and basic Lewis site at the same time [67], [68]. After overnight acetone adsorption on Pt/CeO_2-ZrO_2 and CeO_2-ZrO_2, the same surface species were observed, and the bands became more intensive (Fig. 7 B). However, when hydrogen was adsorbed before the exposure of the samples to acetone, significant changes in the spectra of Pt/CeO_2-ZrO_2 and CeO_2-ZrO_2 were obtained. The intensity of the spectrum detected after 5 min of acetone adsorption on the Pt/CeO_2-ZrO_2 catalyst is much lower compared to CeO_2-ZrO_2 (Fig. 7 A). The predominant species on the surface of 1Pt/CeO_2-ZrO_2 are acetone adsorbed on L sites through the C=O group (1690 cm^{-1}), MO-L species (1600 cm^{-1}) and enol species (1560 cm^{-1}), whereas no bands for carboxylate structures are observed, while for CeO_2-ZrO_2 sample the main adsorbed species are Ac-L (1690 cm^{-1}) and DAA-L (1627 cm^{-1}). The lower intensity of the spectrum recorded on Pt/CeO_2-ZrO_2 in the presence of H_2 can be explained by the hydrogenation reaction of acetone to i-PrOH with an insignificant amount of aldol-condensation products formed. When all adsorbed hydrogen is consumed for the hydrogenation reaction after 17 h of acetone adsorption, the intensity of the spectra recorded on Pt/CeO_2-ZrO_2 increased to the values of the spectra observed for the pure CeO_2-ZrO_2 sample and Pt/CeO_2-ZrO_2 without hydrogen adsorption (in contrast to the Pt/SiO_2 catalyst) (Fig. 7 B). The bands correspond to Ac-L (1709, 1690 cm^{-1}), DAA-L (1624 cm^{-1}) and again we can see the band at 1580 cm^{-1} attributed to a carboxylate type of acetone adsorption on the catalyst surface. The only reaction on the surface of 1Pt/CeO_2-ZrO_2 after overnight acetone adsorption is acid L-sites catalyzed aldol condensation of acetone to DAA, thus resembling the spectrum obtained without hydrogen pretreatment of the catalyst. On CeO_2-ZrO_2 after 17 h of acetone adsorption in the presence of H_2, the surface species were the same as after 5 min of acetone adsorption, i. e. Ac-L and DAA-L. This implies that the reducible oxide support readily participates in the reaction when Pt NPs provide active hydrogen. Possibly, Ce^{3+} formed by partial reduction of the support with spillover hydrogen gives rise to MO formation. The occurrence of aldol condensation implies the availability on the surface of acidic (L-sites) and basic sites (surface –OH group or $–O^{2-}$) in a close proximity functioning in a concerted fashion [64]. The DRIFT spectra of acetone with or without pre-adsorbed hydrogen on 1Pt/ZrO_2 and 1Pt/CeO_2 resemble the intermediate state between Pt/SiO_2 and Pt/CeO_2-ZrO_2. The adsorption behaviour of acetone on Pt/ZrO_2 is close to that on Pt/SiO_2, while the spectra of acetone adsorption on Pt/CeO_2 are closer to Pt/CeO_2-ZrO_2 (Fig. 5). This is in a perfect agreement with the catalytic data. It should be also noted that on supports SiO_2 and CeO_2-ZrO_2, despite that they are both not active in hydrogenation reaction under used ambient conditions, acetone adsorption spectra significantly differ.

According to the results obtained, we can propose a possible scheme of the hydrogenation reaction of carbonyl compounds on a novel 1%Pt/CeO_2-ZrO_2 catalyst (Scheme 2). In the proposed scheme of the reaction, we made several assumptions:

1) Hydrogen can dissociate on the surface of Pt NPs;
2) the rate of the reaction depends on the electronic effects of the substituent group as we showed in this work for p-substituted benzaldehydes (Table 3), thus one of the possible ways of the reaction is nucleophilic hydrogenation which implies hydrogen heterolytic dissociation with formation of H^- and H^+ surface species and H^- attacks the C atom in the C=O group as a nucleophile. The possibility of heterolytic hydrogen dissociation on Pt and hydrogenation of C-O bond by nucleophilic H^- addition was discussed in [69], [70];
3) Addition of nanosized amorphous ZrO_2 to CeO_2 provides an extra number of defects, which act as active sites for substrate adsorption;
4) Lewis acid-base pair sites can stabilize H^- and H^+ species [42], [71];
5) Hydrogen pre-adsorbed on the catalyst surface provides partial support reduction with formation of Ce^{3+}, i.e. an additional amount of Lewis acid sites in a close proximity of Pt for substrate adsorption.
6) carbonyl compound can adsorb on the catalyst surface directly through linear carbonyl coordinated to L-site and through carboxylate-like species (bridged form) coordinated to Lewis acid and basic sites, which was observed in DRIFT spectra of acetone taken as a test molecule.

The general schematic steps of the reaction are shown in Fig. 10.

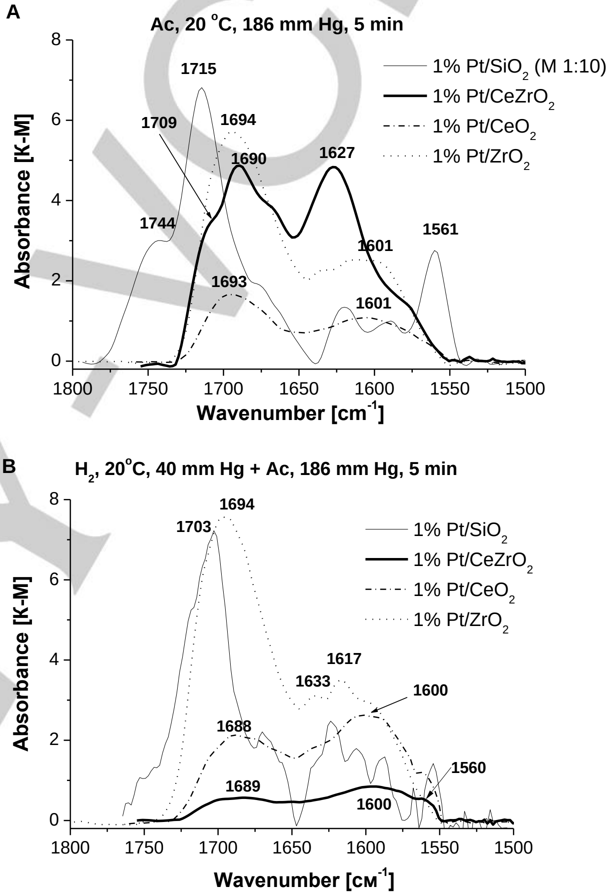

Figure 5. DRIFT spectra of adsorbed acetone on pre-evacuated catalysts (A) and after pre-adsorbed hydrogen (B).

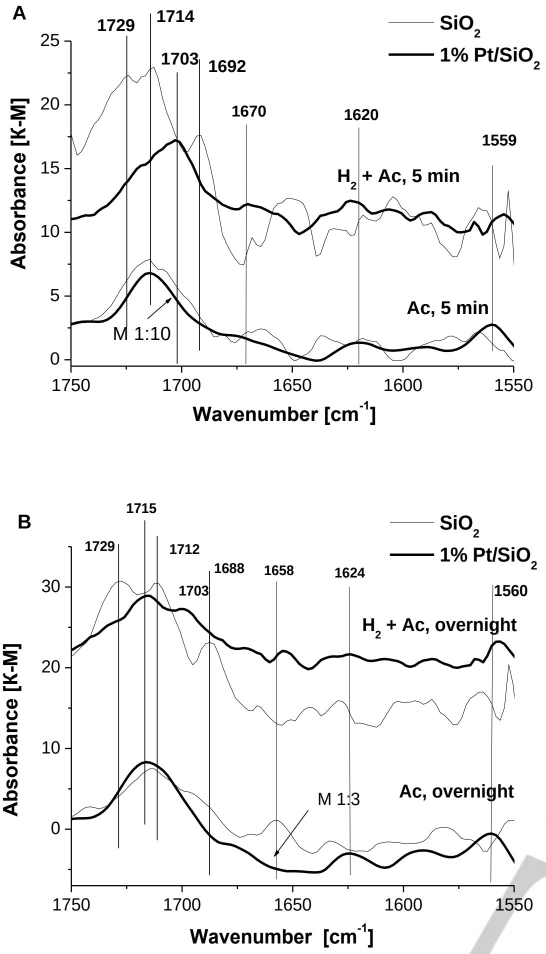

Figure 6. DRIFT spectra of acetone adsorbed for 5 min (A) or 17 h (B) on the pre-evacuated 1%Pt/SiO_2 catalyst and pure SiO_2 before and after pre-adsorbed hydrogen.

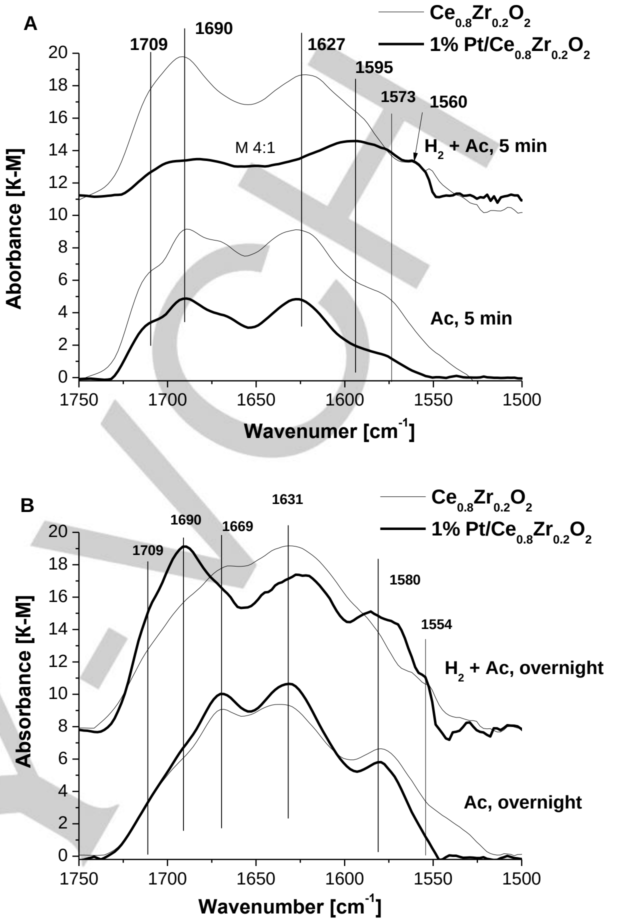

Figure 7. DRIFT spectra of acetone adsorbed for 5 min (A) or 17 h (B) on the pre-evacuated 1%Pt/CeO_2-ZrO_2 catalyst and pure CeO_2-ZrO_2 before and after pre-adsorbed hydrogen.

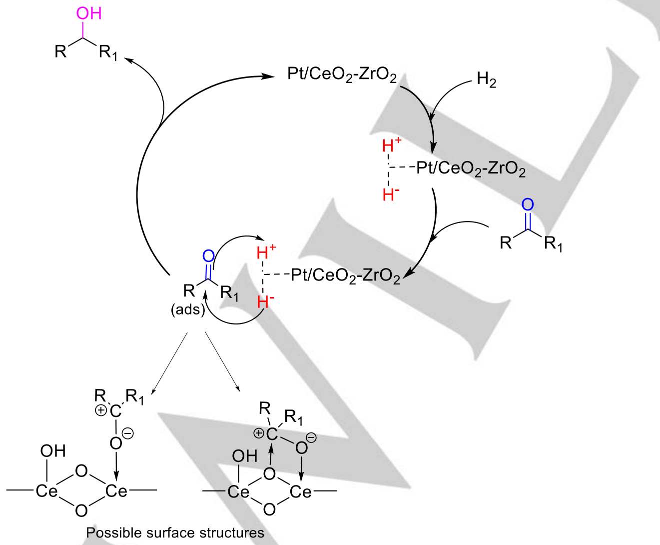

Scheme 2. The possible scheme of carbonyl compounds hydrogenation over Pt/CeO_2-ZrO_2 catalysts.

Conclusions

We prepared a new highly efficient catalytic system, Pt/CeO_2-ZrO_2, which is able to initiate an extremely intensive hydrogen spillover at temperatures from -50°C to +25°C observed by the TPR-H_2 method. The split-over hydrogen was used in selective low-temperature reduction of various carbonyl compounds to the corresponding saturated and α,β-unsaturated alcohols with yields up to 100% at temperatures from -15°C to RT under an H_2 atmospheric pressure, with the Pt content in the reaction mixture being 0.85% mol.

The activity and selectivity of the developed catalysts exceeded those of Pt supported on CeO_2 and ZrO_2 with the same texture characteristics. Moreover, the prepared catalyst is much more active than the commonly used commercial Pd/C catalyst and Pt supported on non-reducible oxide SiO_2 by more than 6 times, clearly indicating the crucial role of the support in the reaction. The proposed hydrogenation protocol is facile: the reaction conditions are much milder than those reported in the literature for homogeneous and heterogeneous catalytic hydrogenation (Supp. Info., See Table S3).

We observed a high selectivity of carbonyl group hydrogenation in the presence of a double C=C bond in cinnamaldehyde over the Pt/CeO_2-ZrO_2 catalyst. We also showed that the rate of the reaction depends on the electronic effects of the substituent group, implying the possibility of nucleophile type hydrogenation of a carbonyl compound. DRIFT experiments showed the differences of the catalysts' behaviour supported on inert (SiO_2, ZrO_2) and active (CeO_2, CeO_2-ZrO_2) carriers for hydrogenation of acetone taken as a probe molecule. According to the results obtained, a possible scheme of the reaction was proposed.

Experimental Section

General materials and methods

^{1} H and ^{13}C NMR spectra were recorded with Bruker AVANCE II 300 (300.1 and 75.5 MHz), Bruker Fourier 300HD (300.1 and 75.5 MHz) and AMXIII 400 (400.1 and 100.6 MHz) spectrometers in $CDCl_3$, DMSO-d_6, and H_2O/D_2O mixture.

TPR measurements were performed in a lab-constructed flow system with a water trap cooled down to -100ºC. The detector (TCD) was calibrated by reduction of CuO (Aldrich-Chemie GmbH, 99%) pretreated in an Ar flow with a gas flow rate of 30 ml min^{-1} at 300ºC. The 1Pt/MeOx catalysts with a weight of 140–170 mg were pretreated in an argon flow with oxygen trap at 250ºC for 90 min. Prior to the TPR experiment, the sample was cooled in an Ar flow to −100ºC using a mixture of ethanol and liquid nitrogen as a cooling agent. Heating from –100 to 850◦C or required temperature was carried out at the rate of 10◦C/min in a 4.6% H_2–Ar gas mixture purified with oxygen trap and supplied with a flow rate of 30 ml min^{-1}. The sample was kept at required temperature (300ºC or 25ºC) until the hydrogen consumption ceased. The experiments were repeated several times for each sample. For TD experiment the sample was cooled after TPR-H_2 in an H_2/Ar flow to −100ºC. TD run was carried out in Ar flow. The obtained data were normalized to 1 g of the sample.

N_2 adsorption-desorption isotherms at 77 K and chemisorption of CO at 35°C were determined using an ASAP 2020 Plus "Micromeritics" system. The BET method was used to calculate the specific surface area (*a*) of the sample. The dispersion of the metal was determined by the irreversible chemisorption of CO. Samples of reduced catalysts before measuring chemisorption were completely restored in an ASAP with hydrogen at 250ºC for 30 min in a stream of pure H_2 (300 ml/min). To determine the irreversible CO chemisorption, two adsorption isotherms were measured — the total isotherm and the isotherm on the carrier. The isotherm on the carrier was determined after pumping out physically adsorbed CO from the sample after measuring the total isotherm. The difference between the two isotherms gives the isotherm of chemisorbed CO. The linear portion of the adsorption isotherm on the metal was extended to intersection with the ordinate axis. The obtained value was taken for a monolayer coating of the metal surface.

The exposed surface of Pt atoms was obtained by chemisorption of CO, and the dispersion was calculated according to the equation:

D= (N_S / N_T) * 100%, where N_S is the number of surface metal atoms, N_T is the total number of metal atoms in the sample.

The number of surface atoms takes into account the stoichiometry of CO adsorption

N_S = F_S * N_m, where N_m is the number of CO atoms in the monolayer; F_S is a stoichiometric factor taking into account the form of CO adsorption on a metal (FS = 1 in the case of linear chemisorption (one CO molecule interacts with one metal atom and FS = 2 in the case of bridge chemisorption - interaction with two metal atoms). The proportion of different forms of CO adsorption is determined from IR spectroscopic data for each specific sample. For studied samples (1%Pt/CeO_2, 1%Pt/ZrO_2, 1%Pt/CeO_2-ZrO_2) the DRIFT-CO spectra showed linear carbonyl adsorption (Figs. S12, SI), FS=1.

The samples morphology was studied using a Hitachi SU8000 field-emission scanning electron microscope (FE-SEM). Before measurements, the samples were mounted on 3 mm copper grids and fixed in a grid holder. The elemental analysis was provided with an EDS system.

The morphology of Pt catalysts was studied using a Hitachi HT7700 transmission electron microscope. Images were acquired in a bright-field TEM mode at 100 kV accelerating voltage. Before measurements, the samples were deposited on 3 mm carbon-coated copper grids from an isopropanol suspension [72]. The average particle size (d_{av}) was calculated as d_{av} = Σ$n_i d_i$/n, where n_i represents the number of particles with the diameter d_i, n is the total number of calculated particles. The number of particles used for calculation of the particle size distribution for each sample was 300, and at least 5 TEM images for the catalyst were used to obtain the statistics of the particle size distribution. Calculation were made using Digimizer Image Analysis Software.

The phase composition of the catalysts and the particle size of the supports were estimated by X-ray diffraction (XRD) analysis. X-ray diffraction patterns were recorded using a DRON-2 diffractometer with Ni-filtered CuKα radiation (λ = 0.1542 nm) in a step scanning mode with the counting time of 0.6 s per step. Identification of the phases was performed by comparison of the position and intensity of the peaks with the data from the files of International Center for Diffraction Data. The crystal size of nanoparticles was calculated from X-ray peak broadening (Scherer's equation).

IR diffuse reflectance spectra (DRIFTS) were recorded at room temperature on a NICOLET "Protege" 460 spectrometer in the range of 6000–400 cm^{-1} with a resolution of 4 cm^{-1}. For a satisfactory signal-to-noise ratio, 500 spectra were stored. The background in the DRIFTS geometry was measured relative to CaF_2 powder dehydrated in a vacuum and sealed in an ampoule. Before measuring the spectra, the samples were subjected to vacuum treatment at a temperature of 250°C for 2 hours. The intensity of the bands in the spectra was expressed in Kubelka-Munk units. Data collection and processing was performed using the OMNIC program. The spectra of adsorbed CO and acetone were presented as the difference between those recorded after and before adsorption.

Acetone adsorption was carried out at room temperature under a saturated vapor pressure of 186 Torr in two ways: 1) on pre-evacuated catalysts and 2) after adsorption of 40 Torr of hydrogen on pre-evacuated catalysts with a subsequent exposure for 30 minutes.

Aldehydes and ketones were purchased from Acros Organics (98%). Solvents (EtOH, Hexane, i-PrOH, THF, Acetone) were of a high purity grade and were used without additional purification.

The reference 1%Pd/AC catalyst was purchased from Acros Organics (S BET 1157, d NPs 2.8±0.7 nm [73]).

10.1002/ejoc.201900215

Catalyst preparation

Support synthesis

The support was synthesized according to the procedure similar to that reported by Kirichenko et al. [31]. To prepare a CeO_2-ZrO_2 (Ce:Zr=0.8:0.2) mixed oxide support (5 g), first the proper amount of $ZrO(NO_3)_2$ (Alfa Aesar, 98+) (1.88 g) was dissolved in an oxalic acid aqua solution (85 ml, 0.49 M, C (Zr) = 45 mg·ml^{-1}) at RT under stirring. Then the solution was poured into 2-propanol (85 ml) to achieve a 1:1 v/v ratio. The final solution was colorless and transparent. A proper amount of $(NH_4)_2Ce(NO_3)_6$ (Alfa Aesar, 98+) (12.75 g) was dissolved in DI water (32 ml). Then 2-propanol (55 ml) was added to the solution to achieve the alcohol to H_2O ratio 1.7:1. The color of the solution changed from light-yellow to dark orange. The co-precipitation of Ce- and Zr-containing solutions was then performed by fast adding the obtained zirconium oxalate alcohol solution to the freshly prepared alcohol Ce salt solution under the control of pH and vigorous stirring. The yellowish precipitate was simultaneously obtained and pH of the mixture decreased to 0.9. After that, pH of the slurry was raised up to 9.2-9.3 by titration with an NH_4OH aqua solution (1.01 M) and kept at this pH for 1 h. The precipitate was then centrifuged and washed by distillated water with further drying in an oven at 80ºC. To investigate the conditions of the formation of the oxide phase, the TG-DTA analysis was performed. The thermograms taken in static air or a He flow are presented in Fig. S1 (SI). The calcination temperature 400ºC (4 h) was chosen according to the TG-DTA data.

ZrO_2 was precipitated from the zirconium oxalate aqua solution mentioned above by titration with an NH_4OH aqua solution (1.01 M) until pH reached 9.2-9.3. Then the slurry was stirred for 1 h. After that, the solid was centrifuged and washed with DI water followed by drying in an oven at 80ºC. The powder was calcined at 800ºC for 2 h to obtain tetragonal ZrO_2, which was proved by XRD (Fig. S3, SI) or calcination was performed at 400ºC for 2 h in a closed crucible.

The preparation of the CeO_2 support included several steps: the required amount of $(NH_4)_2Ce(NO_3)_6$ was dissolved in distilled water at a concentration of 2.5 ml of water per 1 gram of compound at room temperature. The resulting solution was diluted with isopropanol (99%) in a ratio of 1.7 ml of isopropanol per 1 ml of the Ce-containing solution. After dilution, the resulting solution was stirred at room temperature for 1 hour. After that, an aqua solution of oxalic acid (2.3 M) diluted with isopropanol (1:1 v/v) was added under vigorous stirring. The pH of the resulting solution was adjusted to 9.15 with NH_4OH aqua solution (24 % wt.). The resulting suspension was stirred for 30 minutes, then filtered on a Büchner funnel and washed with deionized water. The precipitate was dried at 70°C for 12 hours and calcined in a muffle furnace at 400°C in air in a closed crucible for 4 h. The BET surface areas of the used support and the average particle sizes are given in Table S1 (SI).

Pt deposition on supports

For the synthesis of 1%Pt/MeO_x (MeO_x=CeO_2-ZrO_2, CeO_2, ZrO_2), an 0.51 mM H_2PtCl_6 aqua solution with pH 3.0-3.4 was titrated with an 0.1 M Na_2CO_3 aqua solution until pH reached 6.9-7.1. After that, a proper amount of the support was added to obtain its concentration in the suspension equal to 1 g L^{-1}. Then the suspension was heated up to 80ºC and stirred for 2-3 h depending on the support oxide used, and pH of the suspension was adjusted to assure complete Pt deposition. The amount of Pt deposited was checked by titration of an aliquot of the parent solution (0.2 ml) with an aqueous solution of $KMnO_4$ (0.02 M). For the CeO_2-supported Pt catalyst (Pt 1% wt), it took 2 hours at pH 7.9-8.0 to obtain complete PtO_x deposition. The complete deposition of PtO_x on CeO_2-ZrO_2 and ZrO_2 (Pt 1% wt) was achieved after 3 h of stirring the suspension at pH 7.0. Then the catalysts were isolated by centrifugation and dried under a vacuum at 40ºC using a rotary evaporator. To obtain metallic Pt NPs, the dried catalysts were reduced in H_2 flow (30 ml/min) at 230ºC for 2 h.

The sample 1%Pt/SiO_2 was prepared by conventional impregnation of SiO_2 (KSKG, Russia, S BET=108 m^2/g, pore volume BJH 0.84 cm^3/g) with H_2PtCl_6 aqua solution (0.0103 M) for 1 h with subsequent sample drying under a vacuum at 40ºC using a rotary evaporator. Then Pt was reduced in H_2 flow (30 ml/min) at 230ºC for 2 h.

Catalytic reaction

The hydrogenation reaction was performed in a glass two-necked flask. Before the reaction started, the catalyst (50 mg, 0.85% mol.) was placed in the reactor and pretreated under an H_2 flow (from an H_2 generator CsvetChrom-8) at a desired temperature (-15- +20ºC) for 30 min. After that, the H_2 flow was switched off and the substrate (0.3 mmol) diluted with a solvent (1.5 ml) was added through the sample valve. The reaction proceeded at a desired temperature (-15-+25ºC) in an H_2 atmosphere typically for two or five hours under stirring (950 rpm) (For experimental setup, see Fig. S11, SI). To run the reaction at temperatures below 0ºC, an ice bath with NaCl was used.

The analysis of the products was performed by GC (Crystal-5000.2) equipped with a capillary column (CR-5, 30 m x 2.5 mm) and a flame-ionization detector (FID) calibrated using solutions of individual substances with known concentrations. The conditions of analysis: t of the column was raised gradually from 60 to 190ºC with the rate 30º/min, temperature of the evaporator was 240ºC, temperature of the detector was 240ºC, career gas - He. The conversion (X) and selectivity (S) were determined by GC:

$$X = (n_o – n_i)/n_0$$

$$S = n_p/(n_o – n_i)$$

n_o – molar amount of a substrate with the initial concentration, n_i – molar amount of a substrate in the reaction mixture, n_p – molar amount of a product in the reaction mixture.

The structure and purity of the products were confirmed by ^1H and ^{13}C NMR spectroscopy. Normally, the products were obtained in a quantitative yield and they were not additionally purified. If needed, the purification of products was performed by preparative TLC (Macherey Nagel Alugram Xtra Sil G/UV$_{254}$) using hexane/ethyl acetate (v/v: 3:1) as an eluent. The product was then extracted from the surface of SiO_2 by acetone and the solvent was evaporated under a vacuum at 40ºC.

Acknowledgments

The work was carried out with a financial support from Russian Science Foundation, grant no. 17-73-20282. Authors thank the Department of Structural Studies of Zelinsky Institute of Organic Chemistry for electron microscopy characterization and possibility to acquire spectra on Bruker Fourier 300HD. Author also thank Dr. Vera D. Nissenbaum for TG-DTA analysis of obtained supports.

Keywords: heterogeneous hydrogenation • room temperature • carbonyl compounds • platinum catalyst • ceria-zirconia mixed oxide

References

[1] J. S. Carey, D. Laffan, C. Thomson, M. T. Williams, *Org. Biomol. Chem*. **2006**, *4*, 2337-2347.
[2] D. A. Greenhalgh and N. S. Simpkins, *Synlett*. **2002**, *12*, 2074-2076.
[3] C. D. Gill; D. A. Greenhalgh and N. S. Simpkins, *Tetrahedron*. **2003**, *59*, 9213-9230.
[4] I. P. Query, P. A. Squier, E. M. Larson, N. A. Isley, T. B. Clark, *J. Org. Chem.* **2011**, *76*, 6452-6456.
[5] T. Taniguchi, D. P. Curran, *Org. Lett.* **2012**, *14*, 4540-4543.
[6] M. C. Bryan, P. J. Dunn, D. Entwistle, F. Gallou, S. G. Koenig, J. D. Hayler, M. R. Hickey, S. Hughes, M. E. Kopach, G. Moine, P. Richardson, F. Roschangar, A. Steven, F. J. Weibert. *Green Chem.* **2018**, *20*, 5082–5103.
[7] X. Tan, G. Wang, Z. Zhu, C. Ren, J. Zhou, H. Lv, X. Zhang, L. W. Chung, L. Zhang, X. Zhang, *Org. Lett.* **2016**, *18*, 1518-1521.
[8] N. Gorgas, B. Stöger, L. F. Veiros, K. Kirchner, *ACS Catal*. **2016**, *6*, 2664-2672.
[9] D. Wei, T. Roisnel, C. Darcel, E. Clot, J.-B. Sortais, *ChemCatChem*. **2017**, *9*, 80-83.
[10] F. Christie, A. Zanotti-Gerosa, D. Grainger, *ChemCatChem*. **2018**, *10*, 1012-1018.
[11] P. Maki-Arvela, J. Hajek, T. Salmi, D. Yu. Murzin, *Appl. Catal. A Gen*. **2005**, *292*, 1-49.
[12] M. Tamura, D. Yonezawa, T. Oshino, Y. Nakagawa, K. Tomishige, *ACS Catal*. **2017**, *7*, 5103-5111.
[13] M. Landry, A. Gellé, B. Y. Meng, C. J. Barrett, A. Moores, *ACS Catal*., **2017**, *7 (9)*, 6128-6133.
[14] V. Ananikov, E. Gordeev, M. Egorov, A. Sakharov, S. Zlotin, E. Redina, V. Isaeva, L. Kustov, M. Gening and N. Nifantiev, *Mend. Commun.,* **2016**, *26*, 365-374.
[15] X. Li, W. Zheng, H. Pan, Y. Yu, L. Chen, P. Wu, *J. Catal.* **2013**, *300*, 9-19.
[16] Y. Yuan, Y. V. Kaneti, M. Liu, F. Jin, D. Kennedy, X. Jiang, J. Huang, A. Yu, *J. Energy Chem.* **2015**, *24*, 660-668.
[17] Y. Fujiwara, Y. Iwasaki, T. Maegawa, Y. Monguchi, H. Sajiki, *ChemCatChem*. **2011**, *3*, 1624-1628.
[18] Y. Ding, X. Li, B. Li, H. Wang, P. Wu, *Catal. Comm.* **2012**, *28*, 147-151.
[19] C. Liu, W. Luo, J. Liu, L. Sun, Y. Yang, G. Liu, F. Wang, W. Zhong, C. Guild, S. L. Suib, *Catal Lett*. **2018**, *148*, 555-563.
[20] H. Rong, N. Zhiqiang, Y. Zhao, H. Cheng, Z. Li, L. Ma, J. Li, S. Wei, Y. Li, *Chem. Eur.J.* **2015**, *21*, 12034-12041.
[21] R. Yao, J. Li, P. Wu, X. Li, *RSC Adv*. **2016**, *6*, 81211-81218.
[22] W. Yu, Y. Wang, H. Liu, W. Zheng, *J. Mol. Catal. A: Chem*. **1996**, *112*, 105-113.
[23] X. Han, R. Zhou, B. Yue, X. Zheng, *Catal. Lett*. **2006**, *109*, 157-161.
[24] R. Maache, R. Brahmi, L. Pirault-Roy, S. Ojala, M. Bensitel, *Top Catal*. **2013**, *56*, 658-661.
[25] L.F. Liotta, A. Longo, G. Pantaleo, G.D. Carlo, A. Martorana, S. Cimino, G. Russo, G. Deganello, *Appl. Catal. B*. **2009**, *90*, 470-477.
[26] H. Zhang, J. Wang, Y. Zhang, Y. Jiao, C. Ren, M. Gong, Y. Chen, *Appl. Surf. Sci*. **2016**, *377*, 48-55.
[27] P. Concepcion, A. Corma, J. Silvestre-Albero, V. Franco, J. Y. Chane-Ching, *J. Amer. Chem. Soc*. **2004**, *126* , 5523-5532.
[28] C. Serrano-Ruiz, A. Sepulveda-Escribano, F. Rodrıguez-Reinoso, D. Duprez, *J. Mol. Catal. A Chem*. **2007**, *268*, 227-234.
[29] S. Damyanova, B. Pawelec, K. Arishtirova, M. V. Martinez Huerta, J. L. G. Fierro, *Appl. Catal. A Gen*. **2008**, *337*, 86-96.
[30] N. Kakuta, Y. Kudo, H. Rachi, H. Ohkita, T. Mizushima, *Top. Catal*. **2007**, *42–43*, 377-380.
[31] O. A. Kirichenko, G. W. Graham, W. Chun, R. W. McCabe, *Stud. Surf. Sci. Catal*. **1998**, *118*, 411-420.
[32] E. A. Redina, K. V. Vikanova. *Rus. J. Phys. Chem. A*. **2018**, *92*, 2374-2378
[33] H. Liang, S. Wu, Y. Hong, S. Li, Y. Chen, X. Yu, D. Ye, *Catal. Lett*. **2014**, *144*, 685-690.
[34] N.S. Priya, C. Somayaji, S. Kanagaraj, *J Nanopart Res.* **2014**, *16*, 2214: 1-10. DOI 10.1007/s11051-013-2214-0
[35] G. Arora, D. S. Aidhy, *J. Mater. Chem. A*. **2017**, *5*, 4026-4035.
[36] B. Feng, I. Sugiyama, H. Hojo, H. Ohta, N. Shibata, Y. Ikuhara, *Sci. Rep.* **2016**, *6*, 20288. DOI: 10.1038/srep20288.
[37] a) R. Krishn, D. M. Fernandes, V. F. Domingos, E. S. Ribeiro, J. C. Gil, C. Dias, J. Ventura, C. Freire, E. Titus, *RSC Adv*. **2015**, *5*, 60658-60666; b) W. Karim, C. Spreafico, A. Kleibert, J. Gobrecht, J. V. Vondele, Y. Ekinci, J. A. van Bokhoven, *Nature*. **2017**, *541 (7635)*, 68-71; c) Clelia Spreafico, Waiz Karim, Yasin Ekinci, Jeroen A. van Bokhoven, Joost Vande Vondele, *J. Phys. Chem. C*. **2017**, *121*, 17862-17872.
[38] T. Baidya, A. Gupta, P. A. Deshpandey, G. Madras, M. S. Hegde, *J. Phys. Chem. C*. **2009**, *113*, 4059-4068.
[39] J. Im, H. Shin, H. Jang, H. Kim, M. Choi, *Nature Comm*. **2014**, *3370*, 1. DOI 10.1038/ncomms4370
[40] W. C. Jr. Conner, J. L. Falconer, *Chem. Rev.* **1995**, *95*, 708-759.
[41] Y. Lykhach, T. Staudt, M. Vorokhta, T. Skála, V. Johánek, K. C. Prince, V. Matolín, J. Libuda, *J. Catal.*, **2012**, 285, 6-9.
[42] G. N. Vayssilov, G. P. Petrova, E. A. Ivanova-Shor, V. A. Nasluzov, Alexei M. Shor, P. St. Petkova, Notker Rösch, *Phys. Chem. Chem. Phys*. **2012**, *14*, 5879–5890
[43] G. Dutta, U. V. Waghmare, T. Baidya, M. S. Hegde, *Chem. Mater*. **2007**, *19*, 6430-6436.
[44] P. Bera, A. Gayen, M. S. Hegde, N. P. Lalla, L. Spadaro, F. Frusteri, F. Arena, *J. Phys. Chem. B*. **2003**, *107*, 6122-6130.
[45] P. Fornasiero, J. Kaspar, T. Montini, M. Graziani, V. Dal Santo, R. Psaro, S. Recchia, *J. Mol. Catal. A Chem*., **2003**, *204–205*, 683-691.
[46] P. Fornasiero, J. Kaspar, V. Sergo, M. Graziani, *J. Catal.* **1999**, *182*, 56-69.
[47] X. Tang, J. Wei, N. Ding, Y. Sun, X. Zeng, L. Hu, S. Liu, T. Lei, Lu Lin, *Renew. Sust. Energ. Rev*. **2017**, *77*, 287-296.
[48] L. Hu, L. Lin, Z. Wu, S. Zhou, S. Liu, *Renew. Sust. Energ. Rev*. **2017**, *74*, 230-257.
[49] J. Han, Y.-H. Kim, H.-S. Jang, S.-H. Hwang, J. Jegal, J. W. Kim, Y.-S. Lee, *RSC Adv*. **2016**, *6*, 93394-93397.
[50] J. Han,Y.-H. Kim, B. Y. Jung, S.-H. Hwang, J. Jegal, J.-W. Kim, Y.-S. Lee, *Synlett*. **2017**, *28*, 2299–2302.
[51] T. Wang, J. Zhang, W. Xie, Y. Tang, D. Guo, Y. Ni, Catalysts, **2017**, *7 (3)*, 92. DOI 10.3390/catal7030092.
[52] N. Ly, K. Al-Shamery, C.-E. Chan-Thaw, L. Prati, P. Carniti, A. Gervasini, *Catal Lett.* **2017**, *147*, 345-359.
[53] M. S. Ide, B. Hao, M. Neurock, R. J. Davis, *ACS Catal*. **2012**, *2*, 671-683.
[54] X. Xiang, W. H. He, L. S. Xie, F. Li, *Catal. Sci. Technol*. **2013**, *3*, 2819-2827.
[55] Z. H. Sun, Z. M. Rong, Y. Wang, Y. Xia, W. Q. Du, Y. Wang, *RSC Adv*. **2014**, *4*, 1874-1878.
[56] Z. Guo, Y. T. Chen, L. Li, X. M. Wang, G. L. Haller, Y. H. Yang, *J. Catal*. **2010**, *276*, 314-326
[57] Z. Y. Guo, C. X. Xiao, R. V. Maligal-Ganesh, L. Zhou, T. W. Goh, X. L. Li, D. Tesfagaber, A. Thiel, W. Y. Huang, *ACS Catal*. **2014**, *4*, 1340-1348.
[58] S. Bhogeswararao, D. Srinivas, *J. Catal*. **2012**, *285*, 31-40.
[59] X. X. Han, R. X. Zhou, B. H. Yue, X. M. Zheng, *Catal. Lett*. **2006**, *109*, 157-161.
[60] Y. Li, P. F. Zhu, R. X. Zhou, *Appl. Surf. Sci*. **2008**, *254*, 2609-2614.
[61] Y. Wang, W. He, L. Wang, J. Yang, X. Xiang, B. Zhang, F. Li, *Chem. Asian J*. **2015**, *10*, 1561-1570.

10.1002/ejoc.201900215

[62] W. Wang, Y. Xie, S. Zhang, X.Liu, M. Haruta, J. Huang, *Catalysts*. **2018**, *8*, 60. DOI:10.3390/catal8020060

[63] W. Hu, K. Yuan, T. Song, D. Wang, X. Zhang, X. Gao, Y. Zou, H. Dong, Z. Tang, *Angew. Chem. Int. Ed.* **2018**, *57*, 5708-5713. DOI 10.1002/anie.201801289, *Angew.Chem*. DOI 10.1002/ange.201801289, 2018.

[64] M. I. Zaki, M. A. Hasan, L. Pasupulety, *Langmuir*. **2001**, *17*, 768-774.

[65] A.A. Davydov in Molecular Spectroscopy of Oxide Catalyst Surfaces, Wiley Interscience Publ., 2003, 466.

[66] M. I. Zaki, M. A. Hasan, F. A. Al-Sagheer, L. Pasupulety. *Langmuir*. **2000**, *16*, 430-436.

[67] H. Miyata, Y. Toda, Y. Kubokawa, *J. Catal*. **1974**, *32*, 155-158.

[68] A. Panov, J.J. Fripiat, *Langmuir*. **1998**, *14*, 3788-3796.

[69] S. García-Fernández, I. Gandarias, J. Requies, F. Soulimani, P. L. Arias, Bert M. Weckhuysen, *Appl. Catal. B. Environ*. **2017**, *204*, 260–272.

[70] S. Triwahyono, T. Yamada, H. Hattori, *Appl. Catal. A Gen*. **2003**, *250*, 65–73.

[71] K. Ebitani, J. Konishi, H. Hattori,.*J. Catal.* **1991**, *130 (1)*, 257-267.

[72] V. V. Kachala, L. L. Khemchyan, A. S. Kashin, N. V. Orlov, A. A. Grachev, S. S. Zalesskiy, V. P. Ananikov, *Russ. Chem. Rev*. **2013**, *82*, 648 - 685.

[73] S. A. Yakukhnov, E. O. Pentsak, K. I. Galkin, R. M. Mironenko, V. A. Drozdov, V. A. Likholobov, V. P. Ananikov, *ChemCatChem*. **2018**, *10*, 1869-1873.

FULL PAPER

Developed Pt/CeO_2-ZrO_2 catalyst demonstrates record low-temperature hydrogen spill-over affording selective hydrogenation of carbonyl compounds to alcohols at room temperature and atmospheric pressure.

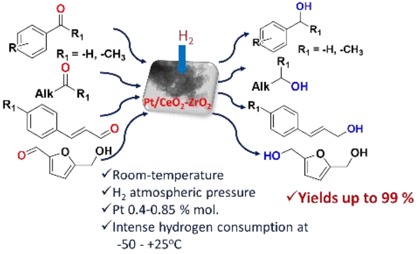

Catalysis, hydrogenation

E. A. Redina, K. V. Vikanova, G. I. Kapustin, I.V. Mishin, O. P. Tkachenko, L. M. Kustov*

Page No. – Page No.

Selective room-temperature hydrogenation of carbonyl compounds under atmospheric pressure over platinum nanoparticles supported on ceria-zirconia mixed oxide